Low-complexity frequency-domain nonlinear equalizer with absolute operation for underwater wireless optical communications

YANTING ZHOU,[1,†] JUNWEI ZHANG,[2,4,†] CHAO LU,[2,3] AND CHANGJIAN GUO[1,5]

[1]*Guangdong Key Laboratory of Optical Information Materials and Technology, South China Academy of Advanced Optoelectronics, South China Normal University, Guangzhou, China*
[2]*Department of Electronic and Information Engineering, The Hong Kong Polytechnic University, Hung Hom, Kowloon, Hong Kong (SAR), China*
[3]*School of Electronics and Information Technology, Sun Yat-Sen University, Guangzhou 510275, China*
[4]*jun-wei.zhang@polyu.edu.hk*
[5]*changjian.guo@coer-scnu.org*
[†]These authors contributed equally to this work.

Abstract: A low-complexity 3rd-order frequency-domain nonlinear equalizer (FD-NLE) with absolute operation is proposed and experimentally demonstrated for underwater wireless optical communications (UWOC). In the proposed FD-NLE scheme, absolute operation and fast Fourier transform (FFT) with multiplication operations are utilized instead of the square and convolution operations used in conventional polynomial nonlinear equalizers (PNLEs), respectively. Therefore, complexity reductions by over 77.3% and 66.9% can be achieved compared with those of PNLE and PNLE with absolute operation, respectively, with a memory length larger than 8. A UWOC system using orthogonal frequency division multiplexing (OFDM) signals with adaptive bit and power loading is also demonstrated to evaluate the performance of the proposed scheme. Experimental results show that data rate increments by $\sim 5.6\%$ and $\sim 5.7\%$ at BER below 7% hard-decision forward error correction (HD-FEC) limit of 3.8×10^{-3}, compared with PNLE and PNLE with absolute operation, respectively, are realized using the proposed scheme. Meanwhile, the proposed scheme has an up to 14.7% complexity reduction compared with conventional frequency-domain PNLE (FD-PNLE), while maintaining similar equalization performance.

1. Introduction

With the development of ocean sensing and communication technologies, demands on underwater wireless communication are further enhanced, as it is crucial for observation and utilization of the underwater world [1]. Although acoustic communication channels have been proved successfully owing to the ability to communicate over kilometers, the limitations of high latency, high transmission losses and varying multi-path propagation still exist. Besides, standard acoustic underwater communications are vulnerable to malicious attacks due to their defects which are mentioned above [2]. Therefore, an upgraded technology is needed to achieve broadband underwater wireless communications and address these problems.

Underwater wireless optical communication (UWOC) systems, which typically use laser diodes (LDs) or light-emitting diodes (LEDs) at 400–700 nm [3,4], have the advantages of high speed, low attenuation, low interference, etc. In addition, the installation and operational costs of UWOC are also lower than other schemes [5,6]. Therefore, the UWOC shows great potential in underwater wireless communication applications.

To further improve the data rate, it has been proposed to use orthogonal frequency-division multiplexing (OFDM) in UWOC systems [7], due to its high spectral efficiency and its ability to cope with severe inter-symbol interferences (ISI) [8]. However, UWOC systems suffer from

several linear and nonlinear distortions resulting from bandwidth-limited transceiver, modulation related nonlinearities and chromatic dispersion (CD) in the water [9,10], which may decrease the transmission performance and limit the achievable capacity. The nonlinear distortions in the UWOC system may arise from various components, such as the modulation nonlinearities of the LD/LED, the electrical amplifiers, and the square-law detection of the photoreceiver [10]. Meanwhile, the high peak-to-average power ratio (PAPR) of OFDM signals may also aggravate the modulation related nonlinearities at the transmitter. To effectively mitigate the linear and nonlinear distortions, 3rd-order Volterra nonlinear equalizers (VNLEs) have been extensively utilized in underwater systems [11,12]. In [11], a sparse 3rd-order VNLE can reduce the bit error ratio (BER) by around half compared with linear equalization at the data rate of 500 Mbit/s. In [12], with simplified 3rd-order VNLE, 3-dB gain of averaged signal-to-noise ratio (SNR) can be achieved as compared with linear equalizer. However, high-order VNLE's superior performance relies on a huge amount of computational complexity, which grows nearly exponentially as the memory length increases and needs high demand for DSP performance and large calculation delay. In order to decrease the computational complexity in VNLE, it has been proved and demonstrated to prune some negligible beating terms such as diagonally pruned VNLEs (DP-VNLEs) or polynomial nonlinear equalizers (PNLEs) in intensity modulation and direct detection (IM/DD) systems [13,14]. In addition, the absolute operation has been introduced to replace the square operation to reduce the complexity of DP-VNLE and PNLE by $20 \sim 40\%$ [13,14]. To further reduce complexity, studies have showed that using low-complexity frequency-domain VNLEs (FD-VNLEs) in OFDM-based visible light communication (VLC) [15] and optical fiber communication [16] systems can avoid the complicated time-domain convolution operations and significantly reduce the computational complexity. More importantly, the computational complexity doesn't change as the memory length increases.

In this paper, to further lower the complexity of nonlinear equalization, we propose and experimentally demonstrate a new form of low-complexity 3rd-order frequency-domain nonlinear equalizer (FD-NLE) based on absolute operation for UWOC systems using OFDM signals. In the proposed scheme, 1) FD-NLE with fast Fourier transform (FFT) and multiplication operations are used to replace the complicated convolution operations in PNLE; 2) absolute operation is used instead of square operation in the PNLE to reduce the complexity of the equalizer. The complexity analysis shows that the computational complexity of the proposed FD-NLE only depends on the symbol size of discrete Fourier transform (DFT) operations, and complexity reductions of more than 77.3% and 66.9% can be achieved, compared with those of 3rd-order PNLE and 3rd-order PNLE with absolute operation, respectively, with a memory length larger than 8. Performance wise, we experimentally demonstrate data rate increments by $\sim 5.6\%$ and $\sim 5.7\%$ at BER below 7% hard-decision forward error correction (HD-FEC) limit of 3.8×10^{-3}, compared with those using PNLE and PNLE with absolute operation, respectively, in a 1-m UWOC link. Meanwhile, the proposed FD-NLE also has an up to 14.7% complexity reduction compared with FD-PNLE (i.e., the FD-VNLE with only self-beating terms), with an only $\sim 0.8\%$ reduction in achieved data rate. Therefore, the proposed FD-NLE scheme offers a significant improvement over existing PNLE schemes in terms of both complexity and performance.

The remaining parts of the paper are organized as follows. In section 2, we inference how to get to the proposed FD-NLE. In section 3, we discuss the experimental setup and results. Eventually, in Section 4, we summarize and conclude this paper.

2. Principle of the proposed frequency-domain nonlinear equalizer with absolute operation

Because of the nonlinearity introduced by amplifiers, LDs and PDs in UWOC systems as well as the interference of light transmission in water, the received signal $r(n)$ can be expressed as a

time-domain Volterra series model:

$$r(n) = \sum_{k_1=0}^{N_1-1} w_1(k_1)x(n-k_1) + \sum_{k_1=0}^{N_2-1}\sum_{k_2=k_1}^{N_2-1} w_2(k_1,k_2)x(n-k_1)x(n-k_2)+$$
$$\sum_{k_1=0}^{N_3-1}\sum_{k_2=k_1}^{N_3-1}\sum_{k_3=k_2}^{N_3-1} w_3(k_1,k_2,k_3)x(n-k_1)x(n-k_2)x(n-k_3) + \ldots\ldots \tag{1}$$

where $x(n)$ is the nth time sample of the transmitted signal, w_b and N_b are the coefficients and memory length of the bth-order term of the nonlinear channel, respectively. To mitigate the linear and nonlinear transmission distortions, VLNE can be implemented as a post-equalizer at the receiver side. The nth sample of the output of the VNLE equalizer can be expressed as:

$$y(n) = \sum_{k_1=0}^{N_1-1} h_1(k_1)r(n-k_1) + \sum_{k_1=0}^{N_2-1}\sum_{k_2=k_1}^{N_2-1} h_2(k_1,k_2)r(n-k_1)r(n-k_2)+$$
$$\sum_{k_1=0}^{N_3-1}\sum_{k_2=k_1}^{N_3-1}\sum_{k_3=k_2}^{N_3-1} h_3(k_1,k_2,k_3)r(n-k_1)r(n-k_2)r(n-k_3) + \ldots\ldots \tag{2}$$

To limit the complexity, the simplest case of 3rd-order VLNE called 3rd-order PNLE can be implemented as a post-equalizer at the receiver side, in which only the self-beating terms are included, thus the complexity as well as the number of coefficients of the nonlinear equalizer can be much reduced. Therefore, the output of the 3rd-order PNLE can be expressed as [14]:

$$y(n) = \sum_{k_1=0}^{N_1-1} h_1{}'(k_1)r(n-k_1) + \sum_{k_2=0}^{N_2-1} h_2{}'(k_2)r^2(n-k_2) + \sum_{k_3=0}^{N_3-1} h_3{}'(k_3)r^3(n-k_3) \tag{3}$$

To lower the complexity, we can then use the absolute operations to replace the square operations of the 2nd-order and 3rd-order nonlinear terms of PNLE. Thus the 3rd-order PNLE with absolute operator can be written as [14]:

$$y(n) = \sum_{k_1=0}^{N_1-1} h_1{}''(k_1)r(n-k_1) + \sum_{k_2=0}^{N_2-1} h_2{}''(k_2)|r(n-k_2)| + \sum_{k_3=0}^{N_3-1} h_3{}''(k_3)|r(n-k_3)|r(n-k_3) \tag{4}$$

where $|\cdot|$ denotes the absolute operator. Applying the Taylor series expansion of $|x|$ around $x=0$, $|x| \approx x^2/2 - x^4/8$ can be obtained when dropping terms higher than 5 [13]. The absolute operation can be realized by an addition and thus reduces the computational complexity [17]. By defining $r_2(n) = |r(n)|$ and $r_3(n) = |r(n)|r(n)$, Eq. (4) can be written as:

$$y(n) = h_1{}''(n) * r(n) + h_2{}''(n) * r_2(n) + h_3{}''(n) * r_3(n) \tag{5}$$

where $*$ is the linear convolution operator. After removing the cyclic prefix (CP) of the received OFDM signal, the temporal sample of each equalized symbol can be written as:

$$y(l) = h_1{}''(l) \otimes r(l) + h_2{}''(l) \otimes r_2(l) + h_3{}''(l) \otimes r_3(l) \tag{6}$$

where $\otimes$ is the circular convolution operator and $l = 0, 1, \cdots M\text{-}1$, M is the DFT size. Note that $h_b{}''$ in Eq. (6) is zero padded up to M taps.

To avoid complicated convolution operations, a low-complexity FD-NLE can then be utilized by transforming Eq. (6) into frequency domain with M-point real-valued FFT:

$$Y(m) = H_1(m)R(m) + H_2(m)R_2(m) + H_3(m)R_3(m) \tag{7}$$

where $R(m)$, $R_2(m)$, and $R_3(m)$ are the M-point real-valued FFT outputs of $r(n)$, $r_2(n)$, and $r_3(n)$, respectively. $H_b(m)$ is the bth-order frequency-domain coefficients, which can be estimated by

least-squares (LS) algorithm [18] based on training symbols. The implementation of the proposed 3rd-order FD-NLE can be realized by parallel 3-tap equalization structure. Note that the FD-NLE can also be applied to PAM modulated systems without CP using an overlap-saved method [18].

The computational complexity of the proposed 3rd-order FD-NLE, which can be evaluated using the required number of real-valued multiplications (RNRM) in one OFDM symbol, was compared with that of frequency-domain linear equalizer (FD-LE), 3rd-order PNLE, 3rd-order PNLE with absolute operation and 3rd-order FD-PNLE. The results with $S = 90$, $M = 512$ and $N_1 = N_2 = N_3 = N$ are summarized in Table 1 and depicted in Fig. 1, where S is the number of data subcarriers. From Table 1 and Fig. 1, the following observations could be made:

(1) The proposed FD-NLE has a reduced complexity compared with the conventional FD-PNLE, since M and $3M$ real-valued multiplications are needed in time domain for the proposed FD-NLE and FD-PNLE, respectively. This complexity reduction becomes more

Table 1. Complexity comparison of different equalizers in one OFDM symbol.

| Equalizer	Operation category	Number of real-valued multiplications
FD-LE	Time domain	0
	FFT [18]	$M(\log_2 M\text{-}3)/2 + 2$
	Frequency domain	$3S$
PNLE	Time domain	$M(N_1 + 2N_2 + 3N_3)$
	FFT	$M(\log_2 M\text{-}3)/2 + 2$
	Frequency domain	0
PNLE with absolute operation [13]	Time domain	$M(N_1 + N_2 + 2N_3)$
	FFT	$M(\log_2 M\text{-}3)/2 + 2$
	Frequency domain	0
FD-PNLE	Time domain	$3M$
	FFT	$3[M(\log_2 M\text{-}3)/2 + 2]$
	Frequency domain	$9S$
Proposed FD-NLE	Time domain	M
	FFT	$3[M(\log_2 M\text{-}3)/2 + 2]$
	Frequency domain	$9S$
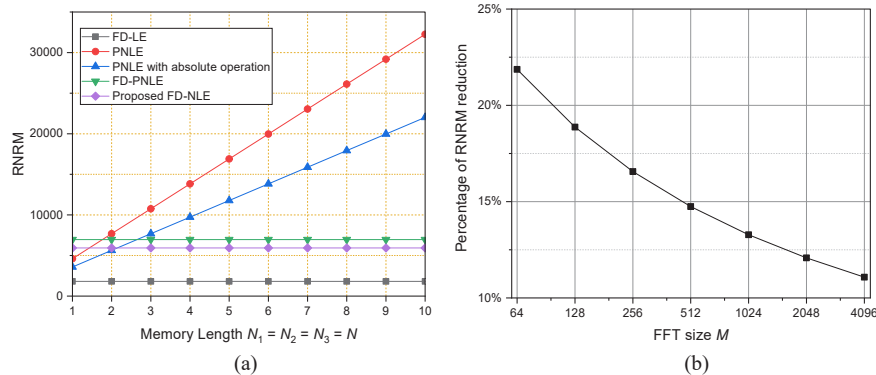
Fig. 1. (a) RNRM versus the memory length of the proposed 3rd-order FD-NLE, FD-LE, 3rd-order PNLE, 3rd-order PNLE with absolute operation and 3rd-order FD-PNLE in one OFDM symbol. (b) Percentage of RNRM reduction of FD-NLE comparing with FD-PNLE versus M at the same transmission bandwidth.

significant when the FFT size is small, with a maximum reduction of up to 22.5%, as shown in Fig. 1(b). In order to reduce the computational complexity while maintaining a reasonable bandwidth allocation flexibility, the FFT size M is set to 512 in our experiment, which corresponding to a 14.7% complexity reduction compared with FD-PNLE.

(2) For time-domain NLE schemes such as PNLE and PNLE with absolute operation, the complexity increases linearly with the memory lengths, while the complexity remains unchanged for frequency-domain equalizers. In fact, proposed FD-NLE and FD-PNLE have less complexity than those time-domain equalizers when the memory length $N > 2$. The proposed FD-NLE can save over 77.3% and 66.9% of real-valued multiplications compared to PNLE and PNLE with absolute operation, respectively, when $N \geq 8$.

(3) From Fig. 1(a) one can also see that the high complexity of PNLE and PNLE with absolute operation mainly come from the convolution operations.

3. Experimental setup and results

3.1. Experimental setup

The performance of the proposed FD-NLE was evaluated in an underwater optical transmission system using OFDM. The experimental setup and digital signal processing (DSP) block diagram are shown in Fig. 2(a). The inverse FFT (IFFT) and CP sizes used for OFDM signal generation were set to 512 and 10, respectively. Besides, the effective payloads were encoded at the 6th to 65th and 67th to 96th subcarriers. In order to avoid the overestimation problem [19], a long random sequence (90 subcarriers, 1000 symbols as 6000 bits for each subcarrier, a total of 540,000 bits) was generated and the training signal was only a small part of it, which guaranteed that the training sequence was distinct from the testing sequence. The OFDM signal was generated via MATLAB and sent to an arbitrary waveform generator (AWG, Tektronix AWG7122C) with a sampling rate of 1.25 Gsa/s. The electrical OFDM signal was then amplified by an electrical amplifier (Mini-Circuits ZHL-32A-S) and combined with an offset driving current via a bias-T before fed into the laser diode (LD, Sharp GH04580A2G) operating at 450 nm. The LD driving current is optimized and set to 46 mA in the experiment, which is in the linear modulation regions of the P-I and V-I curves as shown in Fig. 2(b). We used pure water as the transmission medium in the UWOC system and we have put an agitator in our water tank to simulate turbulence situation in nature. In order to avoid reflections from the multi-layer glass, the incident angle is not typically vertical, so that the reflections from the multi-layer glass wouldn't be received by the PD. After 1-m underwater transmission in a water tank, the optical signal was detected using a photo detector (PD, Hamamatsu C12702). Finally, the received electrical signal was captured by a real-time oscilloscope (Tektronix DPO73304D) operating at 1.25 GSa/s. The off-line DSP included resampling, timing synchronization, serial-to-parallel conversion, equalization with proposed FD-NLE, demapping and error counting. The equalizer coefficients were first estimated by a LS algorithm using 100 training symbols in each subcarrier and remain unchanged in equalization process.

3.2. Experimental results and discussion

Firstly, the driving voltage of the OFDM signals was characterized and optimized by adjusting the AWG-output amplitude at a received optical power (ROP) of -0.7 dBm. 64-QAM signals were modulated in each OFDM frame. Figure 3(a) shows the measured averaged SNR as a function of the AWG-output amplitude using different equalizers with $N_1 = N_2 = N_3 = 8$. It can be seen that increasing the AWG-output amplitude can improve the SNR of all equalizers before the nonlinear effects become dominant. The optimized AWG output amplitudes were found to be 0.75 V, 0.8 V, 0.8 V, 0.9 V and 0.9 V for FD-LE, 3rd-order PNLE, 3rd-order PNLE with absolute
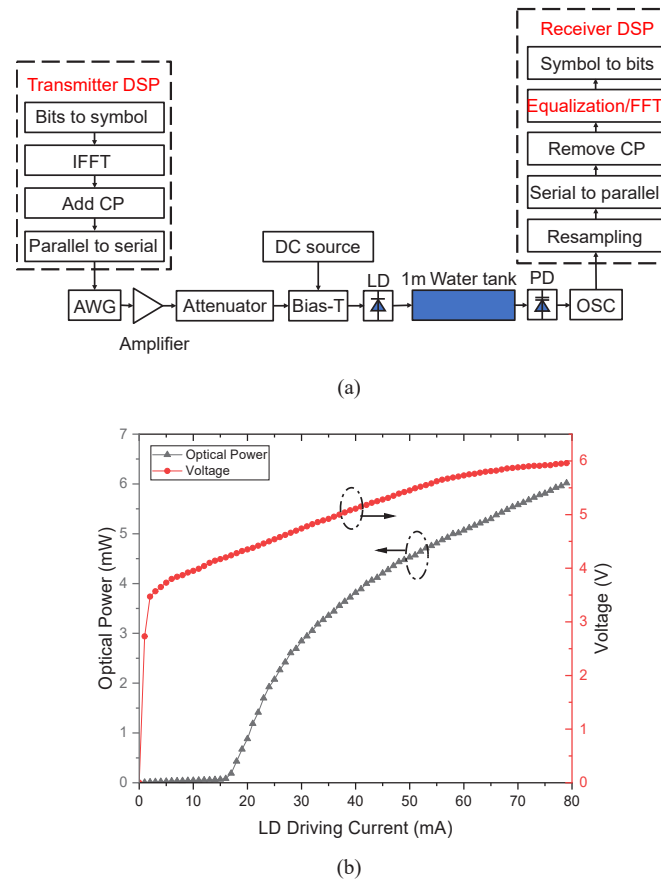
(a)

(b)

Fig. 2. (a) Experimental setup and DSP block diagram. (b) The output optical power and the forward voltage as a function of the LD driving current working at 25 °. AWG: arbitrary waveform generator; LD: laser diode; PD: photo detector; OSC: real-time oscilloscope.

operation, 3rd-order FD-PNLE and proposed 3rd-order FD-NLE, respectively. These values were applied to each equalization scheme in the following experiments. Moreover, it can be seen from Fig. 3(a) that using the 3rd-order FD-NLEs can improve the average SNR by approximately 1 dB compared with 2nd-order FD-NLEs, so we use 3rd-order FD-NLEs in our following experiments.

We then investigated the required memory lengths of different equalizers at a ROP of -0.7 dBm. For the sake of fairness of comparison, memory lengths of all equalizers were set as $N_1 = N_2 = N_3 = N$. Measured BERs as a function of the memory length N for different NLEs using 64QAM-OFDM signal are shown in Fig. 3(b). It can be seen that: 1) Increasing the memory length helps to improve the BER performance of the PNLEs until a BER floor is reached at a memory length of 8. 2) Due to the introduction of higher-order nonlinear terms using absolute operations, the BER performance of PNLE with absolute operation is slightly worse than that of conventional PNLE when the memory length is sufficiently large. Also, the BER performance of proposed FD-NLE is slightly worse than that of FD-PNLE. 3) The BER performance of the proposed FD-NLE and FD-PNLE is better than the PNLEs, which is attributed to the mitigation of high-frequency noise in coefficient estimation and equalization processes in frequency domain. To balance the complexity and performance, N_1, N_2 and N_3 are set to 8 for PNLEs in the following experiments. It should be noted that the values of N_1, N_2 and N_3 depend on the underwater channel and the transceivers and can be much more significant when nonlinear devices (e.g.,
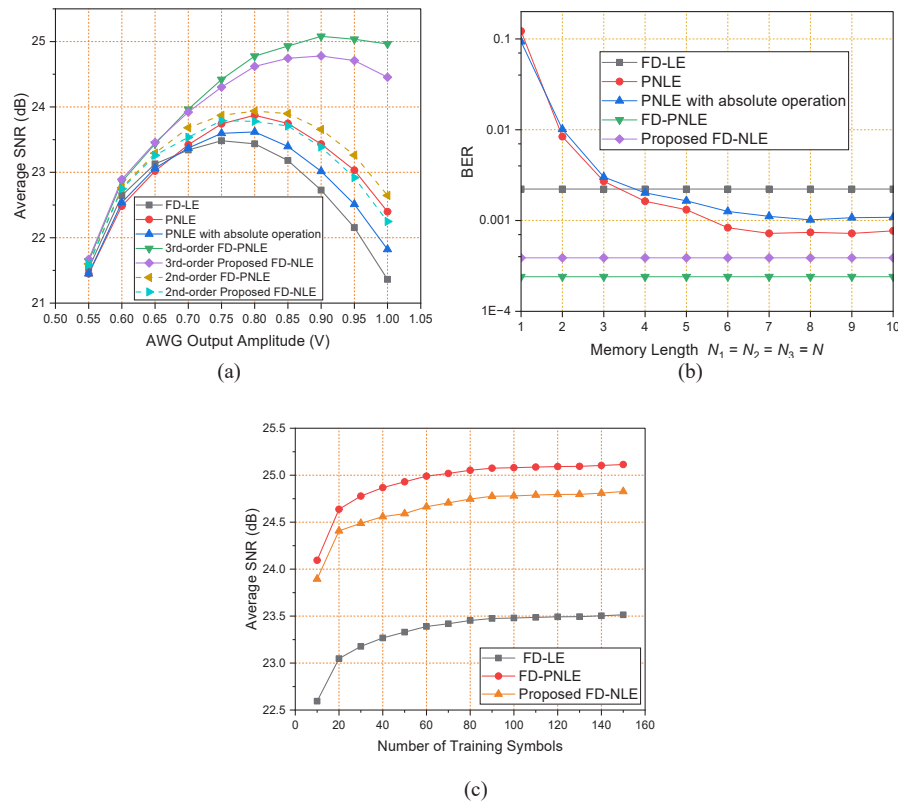
Fig. 3. (a) Average SNR as a function of AWG-output amplitude using different equalizers. (b) Measured BER as a function of memory length using different equalizers. (c) Average SNR as versus the number of training symbols for different frequency-domain equalizers.

silicon photomultipliers) are used [20]. After the above parameters are determined, RNRM can be calculated through Table 1 that the proposed FD-NLE can significantly save ~77.3%, ~66.9% and ~14.7% of real-valued multiplications compared to PNLE, PNLE with absolute operation and FD-PNLE, respectively. It should be also noted that other modulation formats (QPSK, 16-QAM, etc.) can also be used to characterize the performance, which can only result in similar SNR results.

The dependence of the average SNR performance on the required number of training symbols for the FD-LE, FD-PNLE, and the proposed FD-NLE was also investigated and presented in Fig. 3(c). One can see that compared with FD-LE, significant SNR gains can be achieved by the FD-PNLE and the proposed FD-NLE, respectively, while the latter reduces the computational complexity. Meanwhile, to achieve the saturated BERs, 100 training symbols are sufficient for the three equalizers, namely convergence. Note that different from the neural network (NN) based nonlinear equalizers requiring a large number of weight coefficients to perform training and equalization, the proposed 3rd-order FD-NLE with a parallel 3-tap structure only needs to train three weight coefficients for each subcarrier, which can essentially avoid the overfitting phenomenon. To balance the training overhead and performance, 100 training symbols were chosen in the experiment.

Later we measured the SNR of the different subcarriers when using the data mentioned before, as shown in Fig. 4. It can be seen that: 1) The SNR of proposed FD-NLE and FD-PNLE are higher

than those of FD-LE and PNLEs. 2) The SNR performance of our proposed FD-NLE is slightly worse than that of the FD-PNLE while the former saves 14.7% real-valued multiplications.
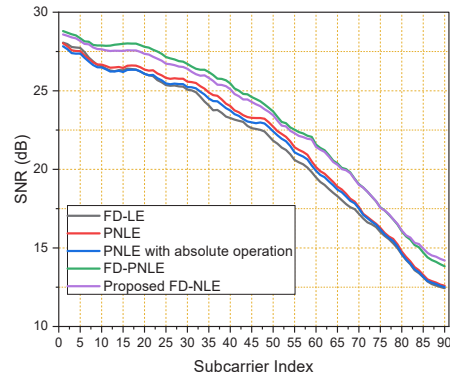

Fig. 4. Measured SNR between subcarriers using different equalizers.

Lastly, bit and power loading were implemented in our experiments to investigate the achievable data rate at 7% HD-FEC limit, as shown in Fig. 5. As can be seen from Fig. 5(a), at the 7% HD-FEC limit of 3.8×10^{-3}, the achievable data rate using the proposed FD-NLE is 1.28 Gbit/s, obtaining increments of data rate by $\sim 5.6\%$ and $\sim 5.7\%$, compared with those using PNLE and PNLE with absolute operation, respectively. Also, it should be noted that, the proposed FD-NLE can save 14.7% RNRM compared with FD-PNLE, with a less than 0.8% data rate penalty.
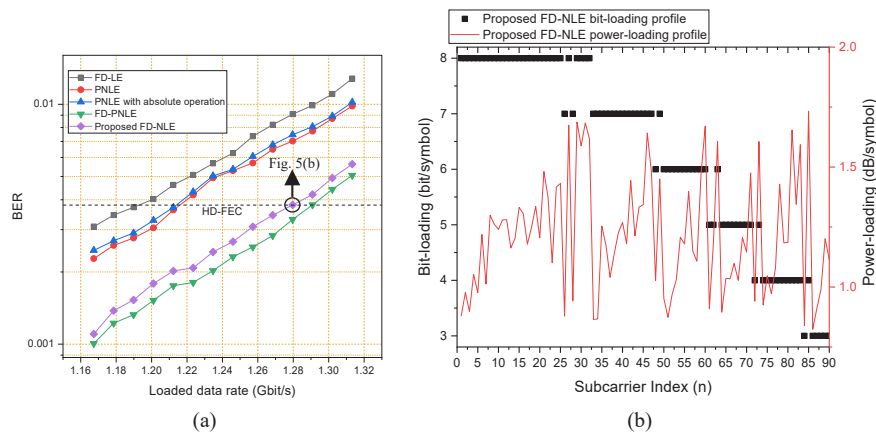

Fig. 5. (a) Measured BER versus loaded data rate. (b) Bit and power loading versus subcarrier index using proposed FD-NLE.

4. Conclusion

In this paper, we have proposed and experimentally demonstrated a low-complexity 3rd-order FD-NLE based on the absolute operation for UWOC using OFDM signals. By replacing the square operation in the conventional PNLE with the absolute one and avoiding complicated convolution operations via frequency-domain equalization, the proposed FD-NLE shows significant lower complexity than those of the PNLE, PNLE with absolute operation, and FD-PNLE. Complexity analysis and experimental results show that the proposed FD-NLE exhibits better performance in both BER and computation complexity as compared with PNLE and PNLE with absolute

operation. Meanwhile, the proposed FD-NLE maintains similar BER performance with that of conventional FD-PNLE, while having a significant complexity reduction.

Disclosures. The authors declare no conflicts of interest.

Data availability. Data underlying the results presented in this paper are not publicly available at this time but may be obtained from the authors upon reasonable request.

References

1. H. Kaushal and G. Kaddoum, "Underwater optical wireless communication," IEEE Access **4**, 1518–1547 (2016).
2. Domingo, "Securing underwater wireless communication networks," IEEE Wireless Commun. **18**(1), 22–28 (2011).
3. L. J. Johnson, "Recent advances in underwater optical wireless communications," Underw. Technol. **32**(3), 167–175 (2014).
4. N. Saeed, "Underwater optical wireless communications, networking, and localization: A survey," Ad Hoc Netw. **94**, 101935 (2019).
5. D. K. Borah, "A review of communication-oriented optical wireless systems," EURASIP J. Wirel. Commun. Networking **2012**(1), 91 (2012).
6. Z. Ghassemlooy, S. Zvanovec, M. A. Khalighi, W. O. Popoola, and J. Perez, "Optical wireless communication systems," Optik **151**, 1–6 (2017).
7. C. Li and Z.Y. Xu, "Experimental Demonstration of Clipping Noise Mitigation for OFDM-Based Underwater Optical Wireless Communications," *Asia Communications and Photonics Conference (ACP)*, Nov. 10-13, 2017.
8. J. Armstrong and B. J. C. Schmidt, "Comparison of asymmetrically clipped optical OFDM and DC-biased optical OFDM in AWGN," IEEE Commun. Lett. **12**(5), 343–345 (2008).
9. N. E. Miroshnikova, G. S. Petruchin, and P. A. Titovec, "Estimation Of The Effect Of Dispersion On The Communication Range In A Wireless Underwater Optical Channel," *Systems of Signal Synchronization, Generating and Processing in Telecommunications*, 2021.
10. C. Ju, N. Liu, X. Chen, and Z. Zhang, "SSBI mitigation in a-RF-tone-based VSSB-OFDM system with a frequency-domain Volterra series equalizer," J. Lightwave Technol. **33**(23), 4997–5006 (2015).
11. Y. Dai, X. Chen, X. Yang, Z. Tong, Z. Du, W. Lyu, C. Zhang, H. Zhang, H. Zou, Y. Cheng, D. Ma, J. Zhao, Z. Zhang, and J. Xu, "200-m/500-Mbps underwater wireless optical communication system utilizing a sparse nonlinear equalizer with a variable step size generalized orthogonal matching pursuit," Opt. Express **29**(20), 32228–32243 (2021).
12. C. Fei, J. Zhang, G. Zhang, Y. Wu, X. Hong, and S. He, "Demonstration of 15-M 7.33-Gb/s 450-nm Underwater Wireless Optical Discrete Multitone Transmission Using Post Nonlinear Equalization," J. Lightwave Technol. **36**(3), 728–734 (2018).
13. Y. Yu, T. Bo, Y. Che, D. Kim, and H. Kim, "Low-complexity nonlinear equalizer based on absolute operation for C-band IM/DD systems," Opt. Express **28**(13), 19617–19628 (2020).
14. Y. Yu, M. R. Choi, T. Bo, Y. Che, D. Kim, and H. Kim, "Nonlinear equalizer based on absolute operation for IM/DD system using DML," IEEE Photonics Technol. Lett. **32**(7), 426–429 (2020).
15. G. Zhang, J. Zhang, X. Hong, and S. He, "Low-complexity frequency domain nonlinear compensation for OFDM based high-speed visible light communication systems with light emitting diodes," Opt. Express **25**(4), 3780–3793 (2017).
16. J. Zhang, C. Guo, J. Liu, X. Wu, A. P. T. Lau, C. Lu, and S. Yu, "Low Complexity Frequency-Domain Nonlinear Equalization for 40-Gb/s/wavelength Long-Reach PON," in *Proc. Proc. Opt. Fiber Commun.*, 2018, Paper W1J.8.
17. S. Chen, "An area/time-efficient motion estimation micro core," IEEE Trans. Consum. Electron. **39**(3), 298–303 (1993).
18. A. Zaknich, *Principles of Adaptive Filters and Self-Learning Systems*, (Springer, Berlin, Germany, 2006).
19. K. Ikuta, Y. Otsuka, Y. Fukumoto, and M. Nakamura, "Overestimation problem with ANN and VSTF in optical communication systems," Electron. Lett. **55**(19), 1051–1053 (2019).
20. X. Hong, J. Du, Y. Wang, R. Chen, J. Tian, G. Zhang, J. Zhang, C. Fei, and S. He, "Experimental Demonstration of 55-m / 2-Gbps Underwater Wireless Optical Communication Using SiPM Diversity Reception and Nonlinear Decision-Feedback Equalizer," IEEE Access **10**, 47814–47823 (2022).